A R C H I V E S O F M E T A L L U R G Y A N D M A T E R I A L S
Volume 57 2012 Issue 1
DOI: 10.2478/v10172-012-0024-5

P.R. SCHELLER*, R. HAGEMANN*

MODEL INVESTIGATIONS ON SLAG ENTRAINMENT IN CONTINUOUS CASTING

MODELOWE BADANIA ZACIĄGANIA ZASYPKI KRYSTALIZATOROWEJ W PROCESIE CIĄGŁEGO ODLEWANIA

Today continuous casting is the state of the art in industrial casting processes. The casting powder used fulfill various tasks such as preventing air contact, absorbing non-metallic inclusions from liquid steel, providing lubrication between strand shell and mould wall and controlling heat transfer. The mould powder in contact with liquid steel surface forms a liquid slag layer. The jet of liquid steel from submerged entry nozzle is reflected at the mould wall forming a lower and upper flow pattern. The upper flow moves along the steel-slag interface and generates shear stress at the interface and waves. Viscosity- and density-differences between the two liquid phases leads under certain flow conditions to finger like protrusions. Reaching a critical flow velocity the protrusions can breakup and form slag droplets following the flow into the liquid steel-pool. These droplets can form finally non-metallic inclusions in steel material, cause defects in the final product and therefore should be avoided. Till now the physical mechanisms of slag entrainment are not completely understood.

The interaction at the liquid-liquid interface was investigated using cold model study using a single-roller driven flow in oil-water systems with various silicon oil properties. The critical values of the dimension free capillary number Ca for droplet breakup marking the start of their entrainment in the lower fluid are determined over a wide-range of fluid properties defined as the product of viscosity ratio (dispersed liquid/continuous liquid) and density ratio (continuous liquid/dispersed liquid) Λ. With the knowledge of thermo-physical properties of steel-slag systems the critical capillary number Ca* for slag entrainment as a function of Λ could be derived. Assuming stable conditions at the interface and no reaction between the phases no slag entrainment should occur under usual casting conditions.

Keywords: continuous casting, slag entrainment, emulsification, slag droplets

Obecnie ciągłe odlewanie jest najnowocześniejszą metodą w przemysłowych procesach odlewania. Zasypka krystalizatorowa stosowana w procesie spełnia różne zadania takie jak: ochrona przed atmosferą powietrza, absorpcja wtrąceń niemetalicznych z ciekłej stali, zapewnienie smarowania między powierzchnią pasma a krystalizatorem oraz kontrola wymiany ciepła. W kontakcie z powierzchnią ciekłej stali zasypka tworzy warstwę ciekłego żużla. Strumień ciekłej stali z wylewu zanurzeniowego jest odbijany od ściany krystalizatora formując zróżnicowane natężenia przepływu. Wyższy przepływ stali wzdłuż powierzchni żużla generuje naprężenia ścinające na powierzchni rozdziału faz oraz jej falowanie. Różnice lepkości i gęstości pomiędzy dwiema ciekłymi fazami prowadzą pod pewnymi warunkami przepływu do powstania wypukłości. Osiągnięcie krytycznej prędkości przepływu może powodować odrywanie wypukłości i formowanie kropelek żużla przepływających do ciekłej kąpieli metalowej. Kropelki te tworzą wtrącenia niemetaliczne w stali, powodując wady w końcowym produkcie, zatem powinno sie dążyć do ograniczenia ich powstawania. Do tej pory fizyczne mechanizmy zaciągania żużla nie zostały dokładnie poznane.

Oddziaływanie na granicy ciecz-ciecz zostało zbadane przy użyciu zimnych modeli z pojedynczą rolką napędzającą w układzie olej-woda, przy użyciu olejów silikonowych o różnych właściwościach. Krytyczna wartość liczby kapilarnej Ca dla rozdrobnienia wskazującego początek zaciągania przy niskim przepływie została wyznaczana dla szerokiego zakresu właściwości na podstawie współczynników lepkości (płyn zdyspergowany/płyn ciągły) i gęstości (płyn ciągły/płyn zdyspergowany) Λ. Znając właściwości termofizyczne układu stal-żużel można wyprowadzić krytyczną liczbę kapilarną Ca* dla zaciągania żużla jako funkcję Λ. Zakładając stabilne warunki na powierzchni międzyfazowej oraz brak reakcji między fazami, w zwykłych warunkach ciągłego odlewania nie powinno następować zaciąganie żużla.

1. Introduction

The emulsification in steel-slag systems is an area of interest in different stages of metallurgy. In the basic oxygen furnace the emulsification of molten steel in top slag or the reverse emulsification of the top slag in the molten steel takes place under certain blowing conditions. These phenomena significantly influence the rate of reaction

* INSTITUTE OF IRON AND STEEL TECHNOLOGY, FREIBERG UNIVERSITY OF MINING AND TECHNOLOGY, D-9596 FREIBERG, GERMANY

between the molten steel and the slag [1],[2]. The effect of sulphur on emulsification behavior in steel was studied by El Gammal *et al.* [3]. Calculating the flotation coefficient they pointed out a maximum of emulsification of steel in slag in the initial stage of desulphurization i.e. at high sulphur content in steel. A theoretical model for the emulsification of slag into steel in gas-stirred ladles was developed by Wei and Oeters [4],[5]. Using a balance of forces acting on fluids near the interface the slag entrainment in steel melt depending on critical flow velocity, drop size and number of droplets formed per time were drawn. In continuous casting process the entrainment of slag in the liquid melt pool is a source for non-metallic inclusions reducing product quality [6]. Increasing casting speed or melt flow rate increases the shear stress in the vicinity of the metal-slag. To get an insight into the mechanism of slag entrainment, model liquids are used to predict the behavior of the steel-slag interface under shear stress conditions. Savolainen *et al.* [7] studied the influence of the thermo-physical properties like density, viscosity and interfacial tension between model liquids on slag entrainment. They pointed out that increasing three parameter, the oil viscosity, density difference and interfacial tension, results in an increase of critical fluid flow velocity needed for slag entrainment. The breakup of droplets of one fluid suspended in a second fluid with density ratio $\rho_c/\rho_d = 1$ induced by velocity lag between the continuous phase and the dispersed droplets was studied in couette-device and four-roller apparatus at low temperatures extensively [8]. The breakup of droplets in a steady shear flow depends on the viscosity ratio η_d/η_c (viscosity of the dispersed phase divided by the viscosity of the continuous phase) and on critical capillary number Ca^*,

$$Ca^* = \frac{u_{crit.}\,\eta_c}{\sigma}. \qquad (1)$$

Here $\eta_c$is continuous phase viscosity, $u_{crit.}$the critical speed in the vicinity of the liquid-liquid interface and σ the interfacial tension between the two liquids. The critical capillary number as a function of the viscosity-ratio describes a border between stable and unstable droplets. Increasing the capillary number to its critical value Ca^* results in droplet breakup producing two or more smaller droplets [11]. In the present work the results of the experimental study for droplet breakup at liquid-liquid interfaces are presented with ρ_c/ρ_d in the range of 1.0 to 1.3 and a wide-range of η_d/η_c using a model with a single-roller.

2. Experimental

2.1. Experimental setup

Figure 1a shows the schematic drawing of the experimental apparatus consisting of a reservoir with roller, driving motor and measuring unit. The rectangular water reservoir with the dimensions $0.2\times0.08\times0.08\ m^3$ is made of acrylic material. Inside of the container a plastic roller with a diameter of *40 mm* and a length of *60 mm* is mounted. The roller is linked to a d.c. motor with controlled rotating speed. *Figure 1b* and *c* shows schematically the arrangement for the study of air entrainment and entrainment of upper liquid in the lower liquid respectively. For the liquid-liquid study the roller is located *10 mm* below the interface in the reservoir and the oil layer thickness is *10 mm* which is carefully stratified. For better visualisation the oil layer is marked by red, oil soluble colour. A high speed camera in front of the acrylic vessel records the process of meniscus formation and droplet breakup with *300 frames per second*.

For analysing of the experiments the open source software *Avidemux* is used. With the help of a mark on the roller and the frame number it is possible to calculate the critical rotation speed $u_{crit.}$ for the first entrained droplet. For each experimental run the water reservoir is covered with new silicone oil. At the start of the experiment the roller rotate with a low rotation speed which is slowly increased by the motor. During the acceleration of the roller a velocity gradient between roller and interface increases and the interface is exposed to an increasing velocity gradient. Reaching $u_{crit.}$ droplet breakup appear. With the observation of the first emulsified droplet the experimental run ends and after a rest time initial conditions for the interface are adjusted and the next run could be started. Using analyse system the critical rotation speed at the time of the first droplet separation and its size was recorded.

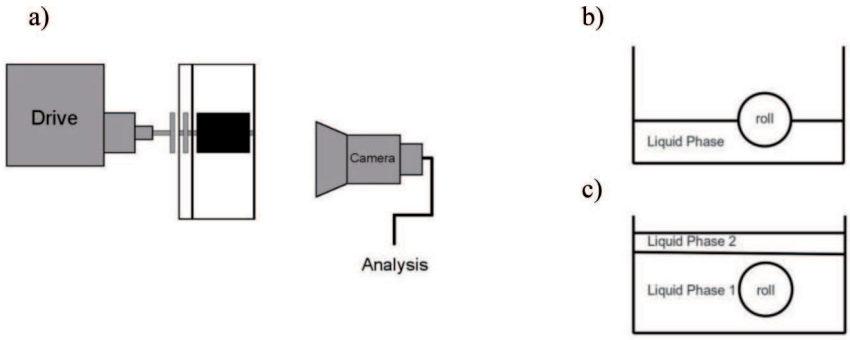

Fig. 1. a) Top view: Configuration of the experimental setup, Side view b) Liquid level for model test c) Liquid level for experiment of upper liquid entrainment

2.2. Dimensionless Analyse

When a liquid-liquid interface is subjected to a shear force from a flow imposed by a rotating roller deformation of meniscus is generated. The flow acts tangentially on the interface leading to deformation and circulation inside of the thin layer. The interfacial tension restore the tendency to breakup of droplets. In order to describe the flow-induced breakup of droplets dimensionless relations are used. Therefore the material properties of the phases and the velocity are related. The utilisation of the Π – *Theorem* [13] leads to a function for the entrainment considering the following variables,

$$\text{Entrainment} = \text{f}\left\{\text{u}_{\text{crit.}}, \rho_\text{c}, \rho_\text{d}, \eta_\text{c}, \eta_\text{c}, \sigma, \text{g}\right\}, \qquad (2)$$

where η_c and η_d are the viscosities of the continuous and disperse phase, u_{crit}. the critical speed in the vicinity of the liquid-liquid interface, σ is the interfacial tension between the two liquids and ρ_c and ρ_d are the densities of the continuous and disperse phase.

Applying the Π – *Theorem* we achieve the Π–groups listed in *Table 1. The reciprocal of* Π_1 is the ratio of the deforming stress exerted by the continuous phase ($\eta_c u_{crit.}$) and the counteracting Laplace pressure ($2\sigma/r$) and is called the capillary number *Ca*. The combination of Π_2 and Π_3 leads to the density-ratio ρ_c/ρ_d and Π_4 is the viscosity-ratio η_d/η_c. The product of η_d/η_c and ρ_c/ρ_d is a dimensionless number describing only material parameters and is called Λ.

TABLE 1

Π-groups

$\Pi_1=\sigma/u_{crit.}\eta_c$	$\Pi_2=u^3\rho_d/\eta_c g$
$\Pi_3=u^3\rho_c/\eta_c g$	$\Pi_4=\eta_d/\eta_c$

2.3. Fluid properties of the model liquids

With the knowledge of Λ for the steel-slag system we can chose the model-liquids for the cold model study. *Table 2 shows the properties of the used Newtonian fluids (density*ρ, dynamic viscosity η and interfacial tension σ).

TABLE 2

Properties of the liquids used for model investigations at 298 K

Liquid	**Phase**	**Density**	**Viscosity**	**Surface tension**	**Interfacial tension against H_2O**	Λ
		[kg m-3]	**[kg m-1 s-1]**	**[N m-1]**	**[N m-1]**	
Silicon oilAk0.65	disperse	760	0,0006	0,016	0,040	1
Silicon oilAk5	disperse	920	0,0046	0,019	0,040	5
Silicon oilAk10	disperse	930	0,0093	0,020	0,040	10
Silicon oilAk35	disperse	955	0,0330	0,021	0,041	34
Silicon oilAk50	disperse	960	0,0480	0,021	0,041	50
Silicon oilAk100	disperse	963	0,0960	0,021	0,042	99
Silicon oilAk200	disperse	966	0,1930	0,021	0,044	199
Silicon oilAk500	disperse	969	0,4850	0,021	0,044	499
Water	continuous	997	0,0009	0,074	–	–

Water was used as continuous phase for all experiments. Silicon oils are used to develop a liquid-liquid interface with differing viscosity-ratios. Through the choice of silicon oils the viscosity was changed in a range of about four magnitudes.

3. Results and discussion

3.1. Model-test

In order to test the roller-device and compare with literature data the entrainment of air by a wet roller (compare Fig. 1b) was investigated using liquids with viscosities ranging over four decades of magnitude. The entrainment data are correlated by the dimensionless *Ca* – number and property number $\Gamma = \delta(\rho \cdot \eta^{-4} \cdot g^{-1})^{\frac{1}{3}}$. In Figure 2 the entrainment data obtained in own study is compared with that obtained by Bolton and Middleman [12]. The air entrainment data in our model are slightly higher than in the study of Bolton and Middleman. This can by related to the differing roller materials and the resulting wetting behaviors between the liquid phase and the roller.

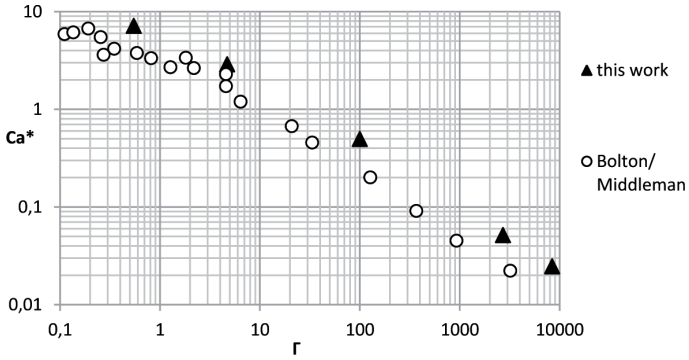

Fig. 2. Air entrainment in roller tests

3.2. Entrainment mechanism and droplet breakup

Figure 3a) to *d*) shows a sequence for entrainment of silicon oil Ak50 in water. With increasing roller-speed a meniscus with finger-like protrusion is formed. Reaching a critical rotation speed droplet breakup takes place, *d*). During droplet breakup the formation of satellite droplets was observed. Up to a viscosity-ratio of $\eta_d/\eta_c > 50$ the length of the finger-like protrusion and thus the possibility of disintegration into more than one droplet increase. *Figure 4a)* to *d*) show the disintegration of a protrusion into a mother droplet with d =14 mm and a satellite droplet (marked by arrow) of only *3 mm* in diameter. The smaller one follows the fluid-flow easily and can be taken away from the interface.

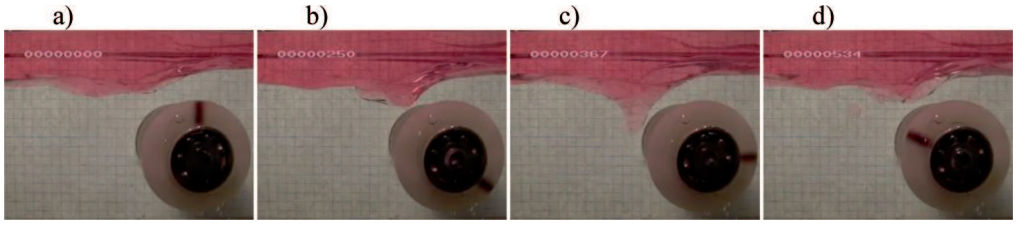

Fig. 3. Meniscus formation and droplet breakup for system silicon oilAk50-water

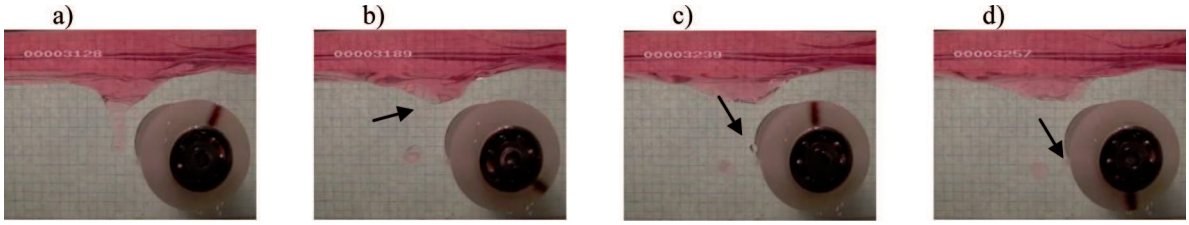

Fig. 4. Formation of satellite droplets

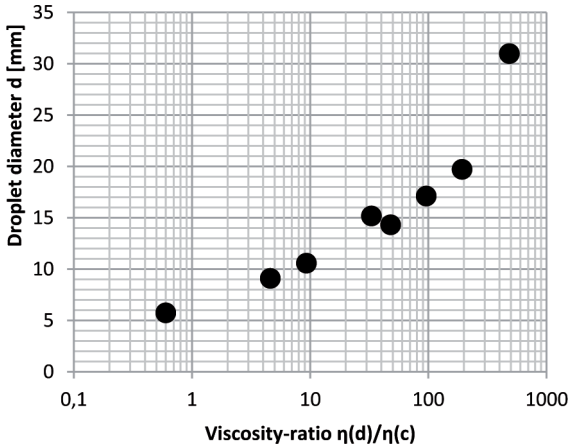

Fig. 5. Effect of viscosity-ratio on the droplet diameter and the critical velocity

3.3. Droplet size

Depending on η_d/η_c the size of the first entrained droplet was measured. Three runs of entrainment experiments were performed for each silicon oil – water system. From the captured picture of the first entrained droplet we derived the area of droplet using the open source program *ImageJ*. Assuming ideally spherical shaped droplets we can calculate the diameter d. Figure 5 shows the droplet diameter as a function of viscosity ratio of the dispersed to continuous phase. With constant interfacial tension we observed an increase in droplet diameter which was also mentioned in other studies [7],[18].

3.4. Correlation between Capillary number and the ratio of viscosity and density

Theoretical and experimental studies of Rallison and Strove [9], [14] pointed out that the breakup of Newtonian fluid droplets entrained in a immiscible fluid depend only on Ca^* and η_d/η_c if inertial effects are negligible. For the model liquids used in our experimental study ρ_c/ρ_d ranged from *1.0–1.3*. In our experiments dependency between Ca^* and 1 should be generalized as $Ca^* = f(1)$ and is plotted in Fig. 6.

The entrainment data correlated by equation 3 is presented in Fig. 6. The data points are dividing the areas of no entrainment (Ca – values below Ca^*) from the area of entrainment of the upper liquid (Ca – values higher then Ca^*). For fixed Λ three data points on breakup were measured. For the range $0.001 < \Lambda < 10$ the critical capillary number is constant. In this region the Ca^* is independent of Λ. For $\Lambda > 10$ the capillary number increases up to 0,038 by value of $\Lambda = 500$. Beyond this value we assume a drastically increase of Ca^* as reported by Strove [14] for high viscosity ratios in a cone-plate device. In Fig. 6 the values of the present study are compared with the data of Savolainen *et al.* [7] performing entrainment experiments with differing density-ratios and interfacial tensions. Considering different model configurations the measured data are in the same range. For constant σ and increasing Λ we observe increasing Ca^*-numbers. The capillary number seems to be very sensitive to interfacial tension. Savolainen *et al.* were using H_2O-Na-Cl-solutions with different Na-Cl concentrations in order to varied ρ_c/ρ_d in a range of *1.1-1.3*. With increasing Na-Cl-content the density-ratio increases but the interfacial tension is diminished. With the results of Salvolainen *et al.* and our own data we assume a strong influence of decreasing interfacial tension on the capillary number for nearly constant Λ. For decreasing σ and constant Λ we assume increasing Ca^*. To prevent entrainment at liquid-liquid interfaces we have to keep the value of Ca lower than Ca^*. Doing so we can either increase slag viscosity resulting in a higher values of Λ or increase interfacial tension σ resulting in lower values of system capillary numbers.

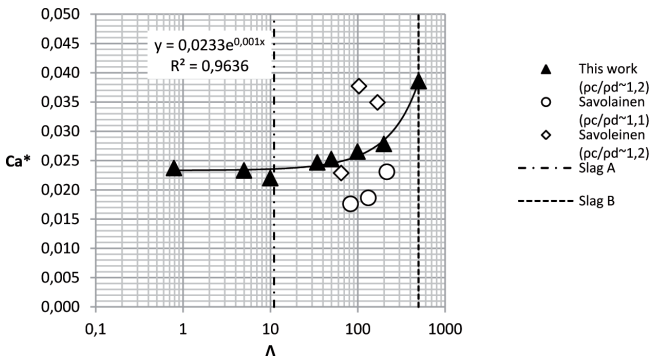

Fig. 6. Entrainment data for droplet breakup at liquid-liquid interfaces

3.5. Considerations on steel-slag systems

To get an insight into the effect of various components on the thermo-physical properties the viscosity of mould slags and the interfacial tension between mould slags and liquid steel was measured. Therefore a slag basic mixture was chosen and the components of interest were changed. The viscosity measurements were carried out using a rotating bob viscometer in combination with a high temperature furnace. The torque of a rotating cylinder immersed in a liquid slag is measured under a constant cooling-rate of *10 K/min*. The viscosity measurements and the related parameters are described elsewhere [15]. The measurements of the interfacial-tension for mould powder in contact with a liquid steel (*DIN100Cr6 – Mat. No. 1.3505*) where

TABLE 3

Values of density, viscosity and interfacial tension for liquid steel and liquid slag at T = 1823 K

Slag	ρ_d [kg m-1]	η_d [Pa s]	σ [N/m]		steel	ρ_c [kg m-1]	η_c [Pa s]	Λ
A	2500	0,02	0,9		100Cr6	6900	0,005	11
B	2600	0,9	1,2					497

performed using the drop weight method, as reported in [16]. The density of the slag was calculated using published relationship [17].

For the steel-slag system the values of ρ_c/ρ_d are in the range of *2.5-2.6* and η_d/η_c is in the range of 4-180. The density-difference between steel and slag produces a counteracting parameter against entrainment as reported by Harman and Cramb [19]. We used the minimum and maximum values of viscosity, density and interfacial tension to calculate the material number Λ (Table 3). These values are marked by vertical lines in Fig. 6. Using the *Ca** - Λ – diagram to predict entrainment of slag into steel we achieve critical capillary numbers *Ca** in the range of *Ca = 0.025-0.045*. If we consider the steel velocity u_{steel} *= 0.3 m/s* in the vicinity of the steel-slag interface and constant interfacial tension the resulting system capillary numbers are in the range of *Ca*= 0.0017-0.002 and are significantly lower compared to the critical value obtained in experimental model investigation. For these conditions with the stable steel-slag interface the droplet breakup should not appear. But in the case of a local decrease of interfacial tension due to reactions at the steel-slag interface the system capillary number increases to higher values. Chung and Cramb [19] reported a number of dynamic interfacial phenomena during their study of interfacial tension between liquid *Fe-11pct Ti* – alloys and liquid slag. They observed a decrease of interfacial tension to σ *= 50 mN/m*. Those low interfacial tensions increase the system capillary number up to *20* times and droplet breakup can appear. We also have to regard that the critical velocity we have measured in the model investigations is related to the speed of a roller in a distance of *10 mm* from the liquid-liquid interface. For the calculation of *Ca**-Λ-diagram we used the critical roller-speed. The real velocity in the vicinity of the interface should be lower. Assuming a velocity gradient the velocities should be lower and the critical capillary numbers for slag entrainment too.

4. Conclusions

Droplet breakup at liquid-liquid interface exposed to a shear flow was investigated at room temperature using a single-roller model and various silicon oil-water-systems. We observed increasing values of the critical capillary number *Ca** with increasing material parameter Λ at constant interfacial tension σ. The droplet diameter of the first entrained droplet increases with increasing Λ and the formation of satellite drops could be observed for $\Lambda > 50$. To keep away from critical capillary numbers we have to enlarge either the material parameter Λ or the interfacial tension σ.

Assuming constant interfacial tension and a metal flow of 0.3 m/s in the vicinity of the steel-slag interface system *Ca - numbers* are in the range of *Ca*= 0.0017-0.002 and no slag entrainment should appear. However the strong change of the interfacial tension because of chemical reactions at the steel-slag interface can lower the interfacial tension and therefore promote the entrainment of slag droplets into steel.

Acknowledgements

This research was supported by the german research foundation (DFG Deutsche Forschungsgemeinschaft), Project Nr 051201019. This is gratefully acknowledged.

REFERENCES

[1] R. Singh, D. Gosh, Ironmaking Steelmaking **17**, 333 (1990).
[2] Q. He, N. Standish, ISIJ International **30**, 356 (1990).
[3] T. Gammal, G. Hinds, U. Schoneberger, Steel Research **62**, 152-156 (1991).
[4] T. Wei, F. Oeters, A model test for emulsification in gas-stirred ladles, Steel Research **62**, 60-68 (1992).
[5] J. Mietz, S. Schneider, F. Oeters, Emulsification and mass transfer in ladle metallurgy, Steel Research **62**, 10-15 (1991).
[6] J. Park, Thermodynamic Investigation on the formation of inclusions containing $MgAl_2O_4$ spinel during 16Cr – Ni austenitic stainless steel manufacturing process, Materials Science and Engineering A **472**, 43-51 (2008).
[7] J. Savolainen, T. Fabritius, O. Mattila, Effect of Fluid Physical Properties on the Emulsification, ISIJ International **49**, 26-36 (2009).

[8] J. J a n s s e n, A. B o o n, W. A g t e r o f, Influence of Dynamic Interfacial Properties on Droplet Breakup in Simple Shear Flow AIChE Journal **40**, 1929-1939 (1994).

[9] J. R a l l i s o n, The Deformation of Small Viscous Drops and Bubbles in Shear Flows, Annu. Rev. Fluid Mech. **16**, 45-66 (1984).

[10] B. G e l f a n d, Droplet Breakup Phenomena in Flows with Velocity Lag, Pro. Energy Combustion Sci. **22**, 202-263 (1996).

[11] H. S t o n e, Dynamics of Drop Deformation and Breakup in Viscous Fluids, Annu. Rev. Fluid Mech. **26**, 65-102 (1994).

[12] B. B o l t o n, S. M i d d l e m a n, Air Entrainment in a Roll Coating System, Chemical Engineering Science **35**, 597-601 (1980).

[13] P. G r a s s m a n n, Physikalische Grundlagen der Verfahrenstechnik (1983), 3.Auflage, Verlag Sauerländer AG, Aarau.

[14] P. S t r o v e, P. V a r a n a s i, An Experimental Study on Double Emulsion Drop Breakup in Uniform Shear Flow, Journal of Colloid and Interface Science **99**, 360-373 (1984).

[15] L. W u, H.P. H e l l e r, P.R. S c h e l l e r, Accuracy of viscosity measurements using rotation viscometer, Procedings of the 9 th Conference on Molten Slags, Fluxes and Salts, 2012 Beijing, China.

[16] E. O z g u r, Q. Y i l d i r i m, B. O s m a n, Analysis of the drop weight method, Physics Of Fluids **17**, 1-13 (2005).

[17] Slag Atlas (1995), 2.Auflage, Verlag Stahleisen GmbH, Düsseldorf.

[18] J. H a r m a n, A. C r a m b, A Study of the Effect of Fluid Physical Properties upon Droplet Emulsification, Steelmaking Conference Proceedings, 773-783 (1996).

[19] Y. C h u n g, A. C h r a m b, Dynamic and Equilibrium Interfacial Phenomena in Liquid Steel-Slag Systems, Metallurgical and Materials Transactions B **31**, 957-971 (2000).

Received: 10 September 2011.